Spatial–temporal wave mixing for space–time conversion

Dan M. Marom, Dmitriy Panasenko, Pang-Chen Sun, and Yeshaiahu Fainman

Department of Electrical and Computer Engineering, University of California, San Diego, 9500 Gilman Drive, La Jolla, California 92093-0407

Received December 3, 1998

A nonlinear optical processor that is capable of true real-time conversion of spatial-domain images to ultrafast time-domain optical waveforms is presented. The method is based on four-wave mixing between the optical waves of spectrally decomposed ultrashort pulses and spatially Fourier-transformed quasi-monochromatic images. To achieve efficient wave mixing at a femtosecond rate we utilize a cascaded second-order nonlinearity arrangement in a β-barium borate crystal with type II phase matching. We use this ultrafast technique to experimentally generate several complex-amplitude temporal waveforms, with efficiency as high as 10%, by virtue of the cascaded nonlinearity arrangement. © 1999 Optical Society of America

OCIS codes: 320.5540, 320.7110, 190.4380, 190.7110.

Optical spatial–temporal-processing techniques have been used in the past decade for ultrafast waveform synthesis.[1–3] The most-efficient approach utilizes spectral filtering of the frequency components of an ultrashort optical pulse. This filtering can be achieved by spatial dispersion of the frequency components in a pulse shaper—a free-space optical setup consisting of diffraction gratings and lenses—and insertion of a spatial mask with the encoded amplitude and phase information into the spectrally decomposed wave (SDW).[1] An alternative approach for generating this spectral filter uses holographic recording of the spatial Fourier transforms (FT's) of an image and a reference point source. The recorded spatial-frequency information serves as a spectral filter for the SDW of an incident ultrashort pulse. The resultant synthesized waveform is a time-scaled version of the spatial image.[4] This approach can be interpreted as a four-wave-mixing process between two waves carrying spatial FT information and two waves carrying the temporal FT information, resulting in the exchange of information between the spatial and the temporal channels. The holographic recording approach is a two-step process, recording of spatial information followed by readout with a temporal signal, and therefore it cannot be operated at ultrafast rates. The performance of the information exchange is determined by the four-wave-mixing mechanism. Thick holograms formed in bulk photorefractive crystals yield high diffraction efficiency, with a long recording time owing to the electron mobility required for building a space-charge field[5] (from tens of microseconds to several minutes). Multiple-quantum-well semiconductor photorefractives can perform holographic recording with microsecond response time,[6,7] yet the result is low diffraction efficiency because of the short interaction length. Ema[8] reported on pulse-shaping experiments with top response time of less than 20 ps when using the large $\chi^{(3)}$ coefficient in the excitonic resonance of ZnSe film (2.4 μm thick). However, increasing the energy-conversion efficiency requires a much longer interaction length. In contrast, the $\chi^{(3)}$ coefficient governing the bound electron nonlinearity in long-interaction-length bulk crystals is inherently small. An alternative arrangement, utilizing cascaded second-order nonlinearities (CSN's), can be used to achieve the equivalent of a four-wave interaction in a medium with a strong $\chi^{(2)}$ nonlinearity.[9]

In this Letter we report what is believed to be the first successful realization of a spatial–temporal processor capable of generating synthesized temporal waveforms at the output, controlled by a spatial-domain image with femtosecond response time and high conversion efficiency. The CSN arrangement consists of a frequency-up process followed by a frequency-down process that satisfies the type II noncollinear phase-matching condition.[10] Nonlinear wave mixing takes place in the Fourier domain of the temporal and the spatial channels (see Fig. 1). The first nonlinear process of the cascade mixes the SDW field, U_1, of an input ultrashort pulse with an envelope denoted $p(t)$ at a center frequency ω_0, and the spatial FT field, U_2, of a quasi-monochromatic wave of frequency ω_0 that is spatially modulated by a one-dimensional image denoted as $m(x)$. These waves can be expressed in space–time coordinates of Fig. 1,

$$U_1(x';t) = \frac{c}{\alpha\lambda_0 f}\, w\!\left(-\frac{ct}{\alpha}\right)\tilde{p}\!\left(\frac{\omega_0 x'}{2\pi\alpha f}\right)\exp\!\left(-j\,\frac{\omega_0 t x'}{\alpha f}\right), \tag{1}$$

$$U_2(x';t) = \frac{1}{\lambda_0 f}\,\tilde{m}\!\left(\frac{\omega_0 x'}{2\pi c f}\right). \tag{2}$$

The optical carrier frequency and the propagation direction terms in Eqs. (1) and (2) have been omitted

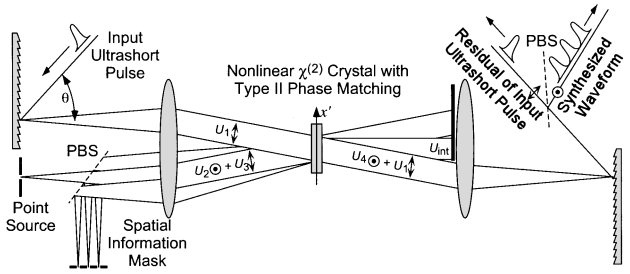

Fig. 1. Experimental setup of the spatial–temporal processor: The CSN results in information exchange in a four-wave-mixing process equivalent. PBS's, polarizing beam splitters.

0146-9592/99/080563-03$15.00/0

for simplicity. The input pupil function of the temporal channel, $w(x)$, sets the time window of the processor in Eq. (1). The functions $\tilde{m}(\cdot)$ and $\tilde{p}(\cdot)$ represent the FT of the spatial mask and the pulse envelope, respectively. The diffraction grating is characterized by the dispersion parameter α [where $\alpha = \sin(\theta)$ and θ is the diffraction angle], c is the speed of light, and f is the focal length of the FT lens. Fields U_1 and U_2 are polarized in the ordinary and the extraordinary directions, respectively, relative to the optical axis of the nonlinear crystal, and their propagation directions satisfy the phase-matching condition. Waves U_1 and U_2 generate an intermediate upconverted wave $U_{\text{int}} \sim \chi^{(2)} U_1 U_2$, which oscillates at sum frequency $2\omega_0$, propagates along the optical axis of the setup, and is polarized in the extraordinary direction.

The second nonlinear process of the cascade mixes the intermediate wave, U_{int}, and the spatial FT of a narrow slit (implementing a one-dimensional spatial Dirac δ function), U_3. The narrow slit in the second spatial channel is illuminated by the same quasi-monochromatic source as U_2 and is copropagating with U_2 after a polarizing beam splitter (see Fig. 1). Wave U_3 is polarized in the ordinary direction and interacts with the extraordinary polarized intermediate wave U_{int}, downconverting the carrier frequency back to ω_0. In this arrangement the phase-matching condition for the downconversion process is automatically satisfied. The resultant wave, $U_4 \sim \chi^{(2)} U_{\text{int}} U_3^*$, propagates in the same directions as U_1 and at the same center frequency but in an orthogonal polarization state. The resultant wave is therefore proportional to the input waves as $U_4 \sim [\chi^{(2)}]^2 U_1 U_2 U_3^*$, which is equivalent to a four-wave-mixing process. The resultant wave can be expressed as

$$U_4(x';t) \propto w\left(-\frac{ct}{\alpha}\right)\tilde{p}\left(\frac{\omega_0 x'}{2\pi\alpha f}\right)\tilde{m}\left(\frac{\omega_0 x'}{2\pi c f}\right) \times \exp\left(-j\,\frac{\omega_0 t x'}{\alpha f}\right)\exp(-j\omega_0 t)\,. \tag{3}$$

Comparing the expression for the resultant wave, expression (3), with the SDW of the input temporal channel, Eq. (1), we can observe that the spatially dispersed frequency components are modulated by the information of the spatial mask. Thus, the femtosecond-rate spatial–temporal processing has generated the SDW of the output temporal optical waveform. Recombining SDW U_4 in the optical setup by use of a second FT lens and grating diffraction yields the output temporal signal

$$y(t) = m\left(\frac{c}{\alpha}\,t\right) \otimes p(t)\,. \tag{4}$$

This synthesized waveform, $y(t)$, is a convolution of the input ultrashort pulse with a space-domain image, whose spatial dependence has been converted to temporal dependence in the spatial–temporal processor. When the duration of the ultrashort pulse is much shorter than the feature size of the temporally mapped mask, $p(t)$ can be approximated by a Dirac δ function, and the output temporal waveform is directly proportional to the information in the mask. If the mask contains fine features, then the output waveform will be a smoothed version of the mask, owing to the convolution operation.

We experimentally demonstrate CSN spatial–temporal wave mixing by use of ultrashort pulses of 100-fs duration at a center wavelength of 800 nm with an energy level of 1 mJ/pulse (generated from a Ti:sapphire ultrashort pulse oscillator combined with a regenerative amplifier). Ten percent of the power of the laser pulse was split off and introduced into the temporal input channel of the processor, generating SDW U_1. The SDW was generated by a 600-line/mm blazed grating (dispersion parameter $\alpha = 0.48$) and a lens of 375-mm focal length. We used the remaining 90% of the pulse power to generate the light source for the implementation of the spatial channels by stretching the pulse width with a grating pair to several-picosecond duration (i.e., generating a chirped pulse), matching the time window of the temporal channel. The stretched pulse was divided into two spatial channels for implementation of waves U_2 and U_3. Since the CSN process occurs with a femtosecond-scale time response because of the fast nonlinearity, a sufficient condition for four-wave-mixing operation is that the field amplitude of the two spatial channels be instantaneously equal. The spatial–temporal wave mixing by the $\chi^{(2)}$ media was performed in a 2-mm-thick type II β-barium borate (BBO) crystal. In our experiment, the entire process was derived from a single pulse from the laser source; thus, the information exchange was done on a single-shot basis. We conducted several experiments to illustrate this real-time processing technique, demonstrating its ability to control amplitude and phase in the output temporal waveform derived from the spatial-information channel.

For initial characterization of the spatial–temporal wave-mixing process through CSN, we focused the two spatial channel waves by use of cylindrical lenses to form line sources at the input spatial channels, generating plane waves U_2 and U_3 in the BBO crystal. Downconverted SDW U_4 was generated only in the presence of the waves from the two spatial channels. The maximum conversion efficiency of input SDW U_1 to filtered output SDW U_4 was 10%, limited by fundamental wave depletion. The conversion efficiency depends on the power of the two spatial-channel waves, as they serve as the pump waves in the CSN process. The high conversion efficiency illustrates the advantage of the CSN approach as opposed to conventional $\chi^{(3)}$ nonlinearity for four-wave mixing.[11]

In our first information transfer experiment we used a mask containing a sequence of narrow slits spaced 0.8 mm apart. We achieved high light throughput by focusing the illuminating beam into the slits with a cylindrical lenslet array. The shaped waveform, consisting of a sequence of pulses, was observed with a real-time pulse-imaging technique[12] (see Fig. 2). As predicted by Eq. (5), the synthesized waveform consists of a sequence of pulses separated by ~1.3 ps. Selectively blocking some of the slits

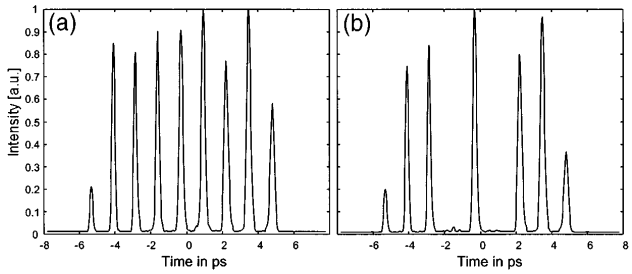

Fig. 2. Synthesized temporal waveform generated by a spatial-information mask consisting of a sequence of equally spaced point sources. (a) All points are illuminated by quasi-monochromatic light. (b) Two point sources are blocked.

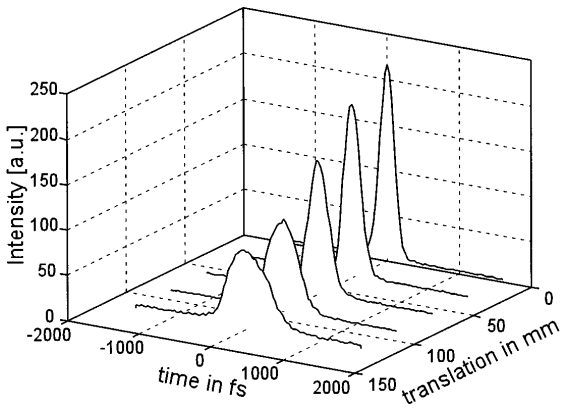

Fig. 3. Synthesized temporal waveforms generated by a quadratic wave front in the spatial channel, generating chirped pulses. The quadratic wave front is generated by longitudinal translation of a point source from the input plane.

resulted in a matching temporal waveform, confirming our ability to perform single-shot temporal waveform synthesis in real-time from a spatial channel. These results were generated under maximal conversion efficiency, at which fundamental wave depletion was observed. Therefore, when some of the slits are blocked, more photons are upconverted by the spatial waves of the open slits, leading to an amplitude distribution change in the pulse sequences of Fig. 2. No evidence of cross talk between channels was detected.

To demonstrate the ability to encode phase information, we used a spatial-information channel that consisted of a variable spherical wave front, generated by longitudinal translation of a cylindrical focusing lens away from the input plane. The spatial-temporal information exchange converted the spatial quadratic phase to the temporal quadratic phase, generating chirped pulses at the output of the processor (see Fig. 3). We estimated the amount of chirp with the pulse imager by use of the technique outlined in Ref. 12, and as expected we found direct correspondence between the longitudinal translation of the focusing lens and the amount of chirp on the synthesized waveform.

Relative to other spatial–temporal processing techniques, the CSN approach provides femtosecond-rate processing, owing to fast bound electron nonlinearity and high efficiency as a result of a relatively large $\chi^{(2)}$ coefficient. The spatial–temporal process that we have demonstrated generates an output temporal waveform that can be reconfigured in real time and is proportional to the convolution of an input ultrashort pulse and a spatial image. Furthermore, wavelength tuning of the synthesized temporal waveform can be achieved by use of different temporal frequencies in the two spatial channels (with a correction to the propagation direction to satisfy phase matching). For operation with pulsed lasers at high repetition rates, the spatial channels can be implemented by use of a second intense cw laser source, or the conversion efficiency of the CSN process should be improved. Since the technique realizes a general four-wave-mixing process of spatial–temporal-information-carrying waves, we can convert the setup to provide the convolution or the correlation signal between spatial and temporal channels, with the output in either the temporal or the spatial domain. Thus, this spatial–temporal process can be considered a fundamental system for performing ultrafast signal processing of optical waveforms in the time and the space domains.

This work was supported in part by the Ballistic Missile Defense Organization, the U.S. Air Force Office of Scientific Research, and the National Science Foundation. Dan Marom acknowledges the support of the Fannie and John Hertz foundation; his e-mail address is marom@kfir.ucsd.edu.

References

1. A. M. Weiner, J. P. Heritage, and E. M. Kirschner, J. Opt. Soc. Am. B **5,** 1563 (1988).
2. P. Emplit, J.-P. Hamaide, and F. Reynaud, Opt. Lett. **17,** 1358 (1992).
3. D. E. Leaird and A. M. Weiner, in *Conference on Lasers and Electro-Optics*, Vol. 6 of 1998 OSA Technical Digest Series (Optical Society of America, Washington, D.C., 1998), p. 99.
4. M. C. Nuss and R. L. Morrison, Opt. Lett. **20,** 740 (1995).
5. P. C. Sun, Y. Mazurenko, W. S. C. Chang, P. K. L. Yu, and Y. Fainman, Opt. Lett. **20,** 1728 (1995).
6. Y. Ding, R. M. Brubaker, D. D. Nolte, M. R. Melloch, and A. M. Weiner, Opt. Lett. **22,** 718 (1997).
7. A. Patrovi, A. M. Glass, D. H. Olsen, G. J. Zydzik, H. M. O'Bryan, T. H. Chiu, and W. H. Knox, Appl. Phys. Lett. **62,** 464 (1993).
8. K. Ema, Jpn. J. Appl. Phys. **30,** L2046 (1992).
9. G. R. Meredith, J. Chem. Phys. **77,** 5863 (1982).
10. M. A. Krumbügel, J. N. Sweetser, D. N. Fittinghoff, K. W. DeLong, and R. Trebino, Opt. Lett. **22,** 245 (1997).
11. J. B. Khurgin, A. Obeidat, S. J. Lee, and Y. J. Ding, J. Opt. Soc. Am. B **14,** 1977 (1997).
12. P. C. Sun, Y. T. Mazurenko, and Y. Fainman, J. Opt. Soc. Am. A **14,** 1159 (1997).